Indoor Particle Concentrations, Size Distributions, and Exposures in Middle Eastern Microenvironments

Hussein, Tareq

2020-01

Hussein , T , Alameer , A , Jaghbeir , O , Albeitshaweesh , K , Malkawi , M , Boor , B E , Koivisto , A J , Londahl , J , Alrifai , O & Al-Hunaiti , A 2020 , ' Indoor Particle Concentrations, Size Distributions, and Exposures in Middle Eastern Microenvironments ' , Atmosphere , vol. 11 , no. 1 , 41 . https://doi.org/10.3390/atmos11010041

http://hdl.handle.net/10138/320568
https://doi.org/10.3390/atmos11010041

atmosphere

MDPI

Article

Indoor Particle Concentrations, Size Distributions, and Exposures in Middle Eastern Microenvironments

Tareq Hussein [1,2,*], Ali Alameer [1], Omar Jaghbeir [1], Kolthoum Albeitshaweesh [1], Mazen Malkawi [3], Brandon E. Boor [4,5], Antti Joonas Koivisto [2], Jakob Löndahl [6], Osama Alrifai [7] and Afnan Al-Hunaiti [8]

1 Department of Physics, The University of Jordan, Amman 11942, Jordan; alameer_hw95@hotmail.com (A.A.); omarjaghbeir@gmail.com (O.J.); kolthoum.baitshaweesh@gmail.com (K.A.)
2 Institute for Atmospheric and Earth System Research (INAR), University of Helsinki, PL 64, FI-00014 UHEL, Helsinki, Finland; joonas.apm@gmail.com
3 Regional Office for the Eastern Mediterranean (EMRO), Centre for Environmental Health Action (CEHA), World Health Organization (WHO), Amman 11181, Jordan; malkawim@who.int
4 Lyles School of Civil Engineering, Purdue University, West Lafayette, IN 47907, USA; bboor@purdue.edu
5 Ray W. Herrick Laboratories, Center for High Performance Buildings, Purdue University, West Lafayette, IN 47907, USA
6 Department of Design Sciences, Lund University, P.O. Box 118, SE-221 00 Lund, Sweden; jakob.londahl@design.lth.se
7 Validation and Calibration Department, Savypharma, Amman 11140, Jordan; olzr27@gmail.com
8 Department of Chemistry, The University of Jordan, Amman 11942, Jordan; a.alhunaiti@ju.edu.jo
* Correspondence: tareq.hussein@helsinki.fi

Received: 11 November 2019; Accepted: 25 December 2019; Published: 28 December 2019

Abstract: There is limited research on indoor air quality in the Middle East. In this study, concentrations and size distributions of indoor particles were measured in eight Jordanian dwellings during the winter and summer. Supplemental measurements of selected gaseous pollutants were also conducted. Indoor cooking, heating via the combustion of natural gas and kerosene, and tobacco/shisha smoking were associated with significant increases in the concentrations of ultrafine, fine, and coarse particles. Particle number (PN) and particle mass (PM) size distributions varied with the different indoor emission sources and among the eight dwellings. Natural gas cooking and natural gas or kerosene heaters were associated with PN concentrations on the order of 100,000 to 400,000 cm^{-3} and $PM_{2.5}$ concentrations often in the range of 10 to 150 $\mu g/m^3$. Tobacco and shisha (waterpipe or hookah) smoking, the latter of which is common in Jordan, were found to be strong emitters of indoor ultrafine and fine particles in the dwellings. Non-combustion cooking activities emitted comparably less PN and $PM_{2.5}$. Indoor cooking and combustion processes were also found to increase concentrations of carbon monoxide, nitrogen dioxide, and volatile organic compounds. In general, concentrations of indoor particles were lower during the summer compared to the winter. In the absence of indoor activities, indoor PN and $PM_{2.5}$ concentrations were generally below 10,000 cm^{-3} and 30 $\mu g/m^3$, respectively. Collectively, the results suggest that Jordanian indoor environments can be heavily polluted when compared to the surrounding outdoor atmosphere primarily due to the ubiquity of indoor combustion associated with cooking, heating, and smoking.

Keywords: indoor air quality; aerosols; particle size distributions; ultrafine particles; particulate matter (PM); smoking; combustion

1. Introduction

Indoor air pollution has a significant impact on human respiratory and cardiovascular health because people spend the majority of their time in indoor environments, including their homes, offices, and schools [1–9]. The World Health Organization (WHO) has recognized healthy indoor air as a fundamental human right [4]. Comprehensive indoor air quality measurements are needed in many regions of the world to provide reliable data for evaluation of human exposure to particulate and gaseous indoor air pollutants [10].

Indoor air pollutant concentrations depend on the dynamic relationship between pollutant source and loss processes within buildings. Source processes include the transport of outdoor air pollution, which can be high in urban areas [11–13], into the indoor environment via ventilation and infiltration, and indoor emission sources, which include solid fuel combustion, electronic appliances, cleaning, consumer products, occupants, pets, and volatilization of chemicals from building materials and furnishings, among others [10,14–28]. Loss processes include ventilation, exfiltration, deposition to indoor surfaces, filtration and air cleaning, and pollutant transformations in the air (i.e., coagulation, gas-phase reactions). Indoor emission sources can result in substantial increases in indoor air pollutant concentrations, exceeding contributions from the transport of outdoor air pollutants indoors. Air cleaning technologies, such as heating, ventilation, and air conditioning (HVAC) filters and portable air cleaners, can reduce concentrations of various indoor air pollutants.

Evaluation of indoor air pollution and concentrations of particulate and gaseous indoor air pollutants in Middle Eastern dwellings has been given limited attention in the literature. In Jordan, one study investigated the effects of indoor air pollutants on the health of Jordanian women [29] and three studies evaluated concentrations of indoor particles in Jordanian indoor environments [30–32]. These studies provided useful insights on the extent of air pollution in selected Jordanian indoor environments and the role of cultural practices on the nature of indoor emission sources. However, these studies did not provide detailed information on the composition of indoor air pollution, including indoor particle number and mass size distributions, concentrations of ultrafine particles (UFPs, diameter < 0.1 μm), and concentrations of various gaseous pollutants.

The objective of this study was to evaluate size-fractionated number and mass concentrations of indoor particles (aerosols) in selected Jordanian residential indoor environments and human inhalation exposures associated with a range of common indoor emission sources prevalent in Jordanian dwellings, such as combustion processes associated with cooking, heating, and smoking. The study was based upon a field campaign conducted over two seasons in which portable aerosol instrumentation covering different particle size ranges was used to measure particle number size distributions spanning 0.01–25 μm during different indoor activities.

2. Materials and Methods

2.1. Residential Indoor Environment Study Sites in Jordan

The residential indoor environments targeted in this study were houses and apartments covering a large geographical area within Amman, the capital city of Jordan (Figure 1). The selection was based upon two main criteria: (1) prevalence of smoking indoors and (2) heating type, such as kerosene heaters, natural gas heaters, and central heating systems. The selected residential indoor environments included two apartments (A), one duplex apartment (D), three ground floor apartments (GFA), and two houses (H). Table 1 lists the characteristics of each study site. All indoor environments were naturally ventilated. The occupants documented their activities and frequency of cooking, heating, and smoking during the measurement campaign.

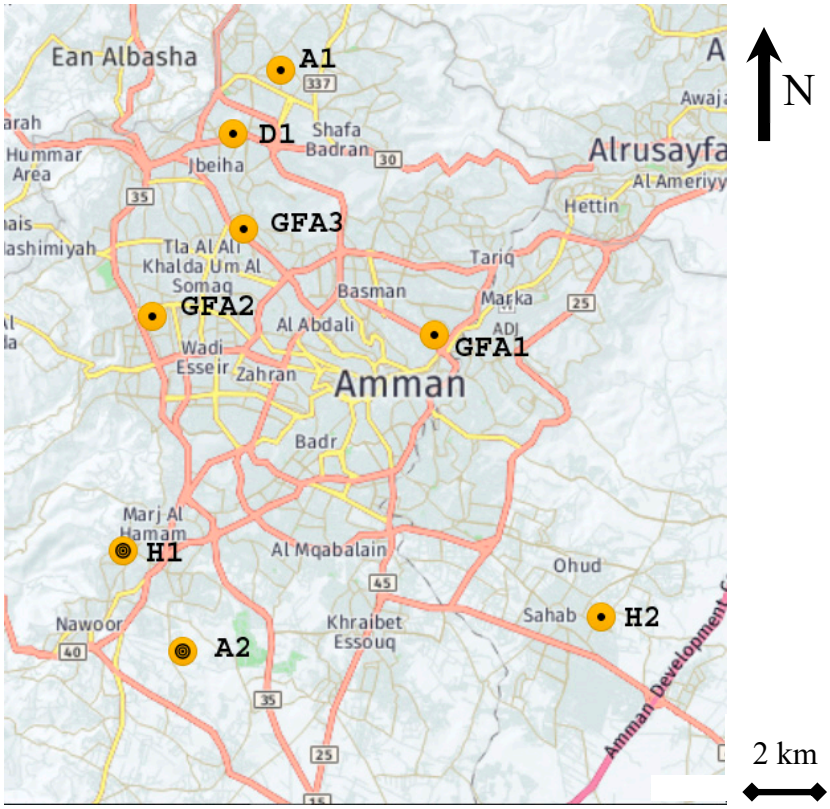

Figure 1. A map showing the Amman metropolitan region with the locations of the selected indoor environment study sites. The type of dwelling is referred to as: (A) apartment, (H) house, (D) duplex apartment, and (GFA) ground floor apartment. Table 1 provides additional details for each dwelling.

Table 1. Characteristics of the selected residential indoor environments. The heating method refers to: kerosene heater (Ker.), natural gas heater (Gas), air conditioning system (AC), electric heaters (El.), and central heating system (Cen.). Cigarette smoking is denoted as (Cig.).

Site ID	Type	Area Type	Kitchen/L. Room	Heating Method					Smoking	
				Ker.	Gas	AC	El.	Cen.	Cig.	Shisha
A1	Apartment (3rd floor)	Suburban	Open	√	√	√				
A2	Apartment (2nd floor)	Rural	Separate			√				
D1	Duplex (2nd and 3rd floors)	Urban Background	Open	√		√				√
GFA1	Ground floor apartment	Urban	Separate	√	√					
GFA2	Ground floor apartment	Urban	Separate				√	√		
GFA3	Ground floor apartment	Urban Background	Open		√				√	√
H1	House	Suburban	Open		√			√		√
H2	House	Rural	Open	√						

2.2. *Indoor Aerosol Measurements and Experimental Design*

2.2.1. Measurement Campaign

Indoor aerosol measurements were performed during two seasons: winter and summer, as indicated in Table 2. The winter campaign occurred from 23 December 2018 to 12 January 2019. All eight study sites participated in the winter campaign. The summer campaign occurred from 16 May to 22 June 2019. Only GFA2, GFA3, and H2 participated in the summer campaign.

Table 2. Measurement periods and lengths of the two campaigns.

Site ID	Winter Campaign			Summer Campaign		
	Start	End	Length	Start	End	Length
A1	13:15, 23.12.2018	11:50, 25.12.2018	1d 22h 35m	–	–	–
A2	18:20, 04.01.2019	19:50, 05.01.2019	1d 01h 30m	–	–	–
D1	14:10, 28.12.2018	22:10, 30.12.2018	2d 08h 00m	–	–	–
GFA1	15:10, 25.12.2018	14:10, 27.12.2018	1d 23h 00m	–	–	–
GFA2	12:00, 09.01.2019	20:40, 12.01.2019	3d 08h 40m	10:30, 13.06.2019	11:20, 22.06.2019	9d 00h 50m
GFA3	12:30, 31.12.2018	18:30, 02.01.2019	2d 06h 00m	18:50, 16.05.2019	23:40, 23.05.2019	7d 04h 50m
H1	20:20, 02.01.2019	16:30, 04.01.2019	1d 20h 10m	–	–	–
H2	12:30, 06.01.2019	15:30, 09.01.2019	3d 03h 00m	20:50, 24.05.2019	21:30, 29.05.2019	5d 00h 40m

2.2.2. Aerosol Instrumentation

Aerosol instrumentation included portable devices to monitor size-fractionated particle concentrations. Supplemental measurements of selected gaseous pollutants were also conducted. The aerosol measurements included particle number and mass concentrations within standard size fractions: submicron particle number concentrations, micron particle number concentrations, PM_{10}, and $PM_{2.5}$. Table 3 provides an overview of the portable aerosol instrumentation deployed at each study site. The use of portable aerosol instruments has increased in recent years, with a number of studies evaluating their performance in the laboratory, the field, or through side-by-side comparisons with more advanced instruments [33–46]. The instruments were positioned to sample side-by-side without the use of inlet extensions. The instruments were situated on a table approximately 60 cm above the floor inside the living room of each dwelling. The sample time was set to 1 min for all instruments, either by default or through time-averaging of higher sample frequency data.

Table 3. List of the portable air quality instruments and the measured parameters.

Instrument	Model	Aerosol Size Fraction	Metric	Performance Ref.
Laser Photometer	TSI DustTrak DRX 8534	PM_{10}, $PM_{2.5}$, and PM_1	Mass	Wang et al. [33]
Personal Aerosol Monitor	TSI SidePak AM520	$PM_{2.5}$	Mass	Jiang et al. [34]
Optical Particle Counter	TSI AeroTrak 9306-V2	D_p 0.3–25 µm (6 bins)	Number	Wang et al. [33]
Condensation Particle Counter	TSI CPC 3007	D_p 0.01–2 µm	Number	Matson et el. [35]
Condensation Particle Counter	TSI P-Trak 8525	D_p 0.02–2 µm	Number	Matson et el. [35]
Gas monitor	AeroQual S500	O_3, HCHO, CO, NO_2, SO_2, TVOC	ppm	Lin et al. [36]

Two condensation particle counters (CPCs) with different lower size cutoffs (TSI 3007-2: cutoff size 10 nm; TSI P-Trak 8525: cutoff size 20 nm) were used to measure total submicron particle number concentrations. The maximum detectable concentration (20% accuracy) was 10^5 cm^{-3} and 5×10^5 cm^{-3} for the CPC 3007 and the P-Trak, respectively. The sample flow rate for both CPCs was 0.1 lpm (inlet flow rate of 0.7 lpm). A handheld optical particle counter (AeroTrak 9306-V2, TSI, MI, USA) was used to monitor particle number concentrations within 6 channels (user-defined) in the diameter range of 0.3–25 µm. The cutoffs for these channels were defined as 0.3, 0.5, 1, 2.5, 10, and 25 µm. The sample flow rate was 2.83 lpm. A handheld laser photometer (DustTrak DRX 8534, TSI, MI, USA) monitored particle mass (PM) concentrations (PM_1, $PM_{2.5}$, respirable (PM_4), PM_{10}, and total) in the diameter range of 0.1–15 µm (maximum concentration of 150 mg/m^3). The sample flow rate for the DustTrak was 3 lpm. A personal aerosol monitor (SidePak AM520, TSI, MI, USA) with a $PM_{2.5}$ inlet was used for additional measurements of $PM_{2.5}$ concentrations. The SidePak is a portable instrument with a small form factor equipped with a light-scattering laser photometer. The CPCs were calibrated in the laboratory [40], whereas the AeroTrak, DustTrak, and SidePak were factory calibrated. Additionally, a portable gas monitor (S500, AeroQual, New Zealand) estimated the concentrations of gaseous pollutants by installing factory calibrated plug-and-play gas sensor heads. The sensor heads included ozone (O_3), formaldehyde (HCHO), carbon monoxide (CO), nitrogen dioxide (NO_2), sulfur dioxide (SO_2), and total volatile organic compounds (TVOCs).

Each instrument was started at different times during the campaigns; and thus, they did not record concentrations at the same time stamp. Therefore, we interpolated the concentrations of each

instrument into a coherent time grid so that we evaluated the number of concentrations in each size fraction with the same time stamp. The built-in temperature and relative humidity sensors used in the aerosol instruments cannot be confirmed to be accurate for ambient observations because these sensors were installed inside the instruments and can be affected by instrument-specific conditions, such as heat dissipation from the pumps and electronics. Therefore, those observations were not considered here.

2.3. Processing of Size-Fractionated Aerosol Concentration Data

The utilization of portable aerosol instruments with different particle diameter ranges and cutoff diameters enables derivations of size-fractionated particle number and mass concentrations [47]: Super-micron (1–10 μm) particle number and mass concentrations, submicron (0.01–1 μm) particle number concentrations, $PM_{2.5}$ mass concentrations, PM_{10} mass concentrations, and PM_{10-1} mass concentrations. Additionally, we derived the particle number size distribution $\left(n_N^0 = \frac{dN}{dlog\left(D_p\right)}\right)$ within eight diameter bins:

- 0.01–0.02 μm via the difference between the CPC 3007 and the P-Trak.
- 0.02–0.3 μm via the difference between the P-Trak and the first two channels of the AeroTrak.
- 0.3–0.5 μm, 0.5–1 μm, 1–2.5 μm, 2.5–5 μm, 5–10 μm, and 10–25 μm via the AeroTrak.

The particle mass size distribution was estimated from the particle number size distribution by assuming spherical particles:

$$n_M^0 = \frac{dM}{dlog\left(D_p\right)} = \frac{dN}{dlog\left(D_p\right)}\frac{\pi}{6}D_p^3\rho_p = n_N^0\frac{\pi}{6}D_p^3\rho_p \quad (1)$$

where n_M^0 is the particle mass size distribution, dM is the particle mass concentration within a certain diameter bin normalized to the width of the diameter range $\left(dlog\left(D_p\right)\right)$ of that diameter bin, dN is the particle number concentration within that diameter bin (also normalized with respect to $dlog\left(D_p\right)$ to obtain the particle number size distribution, n_N^0), D_p is the particle diameter, and ρ_p is the particle density, here assumed to be unit density (1 g cm^{-3}). In practice, the particle density is size-dependent and variable for different aerosol populations (i.e., diesel soot vs. organic aerosol); therefore, size-resolved effective density functions should be used. However, there is limited empirical data on the effective densities of aerosols produced by indoor emission sources. Thus, the assumption of 1 g cm^{-3} for the particle density will result in uncertainties (over- or underestimates, depending on the source) in the estimated mass concentrations.

The size-fractionated particle number concentration was calculated as:

$$PN_{D_{p2}-D_{p1}} = \int_{D_{p1}}^{D_{p2}} n_N^0(D_P)\cdot dlog(D_P) \quad (2)$$

where $PN_{D_{p2}-D_{p1}}$ is the calculated size-fractionated particle number concentration within the particle diameter range D_{p1}–D_{p2}. Similarly, the size-fractionated particle mass concentration $\left(PM_{D_{p2}-D_{p1}}\right)$ was calculated as:

$$PM_{D_{p2}-D_{p1}} = \int_{D_{p1}}^{D_{p2}} n_M^0(D_P)\cdot dlog(D_P) = \int_{D_{p1}}^{D_{p2}} n_N^0(D_P)\frac{\pi}{6}D_p^3\rho_p\cdot dlog(D_P) \quad (3)$$

$PM_{2.5}$ and PM_{10} can be also calculated by using Equation (3) and integrating over the particle diameter range starting from 10 nm (i.e., the lower cutoff diameter according to our instrument setup) and up to 2.5 μm (for $PM_{2.5}$) or 10 μm (for PM_{10}).

3. Results

3.1. Comparisons between Different Aerosol Instruments—Technical Notes

The co-location of different aerosol instruments covering similar size ranges provides a basis to compare concentration outputs as measured through different techniques. First, the $PM_{2.5}$ and PM_{10} concentrations reported by the DustTrak can be compared to evaluate the contribution of the submicron fraction to the total PM concentration in Jordanian indoor environments. According to the DustTrak measurements, it was observed that most of the PM was in the submicron fraction as the mean $PM_{10}/PM_{2.5}$ ratio was 1.03 ± 0.04 (Figure 2). This was somewhat expected as most of the tested indoor activities in this field study were combustion processes (smoking, heating, and cooking) that produce significant emissions in the fine particle range. However, more sophisticated aerosol instrumentation would be needed to verify this finding, such as an aerodynamic particle sizer (APS) and scanning mobility particle sizer (SMPS).

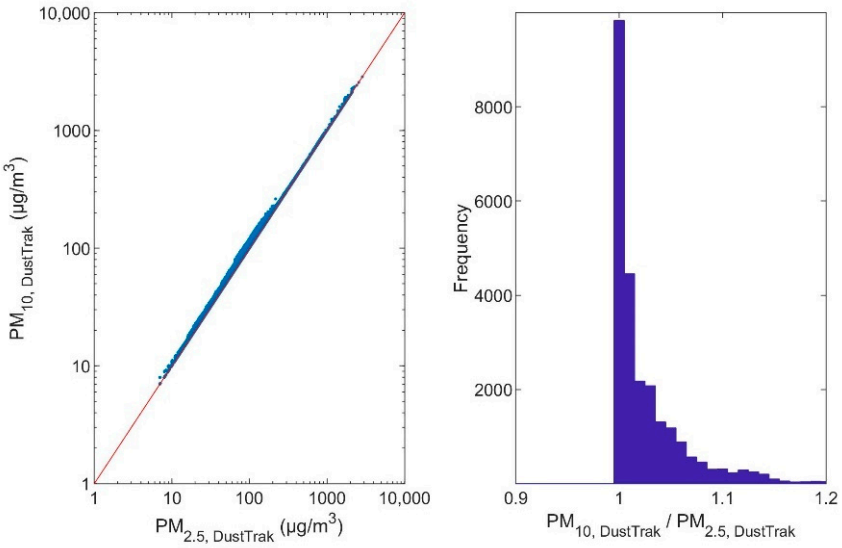

Figure 2. Comparison between the PM_{10} and $PM_{2.5}$ concentrations measured with the DustTrak.

The DustTrak and SidePak both employ a light-scattering laser photometer to estimate PM concentrations. As such, their output can be compared for the same particle diameter range. In general, the $PM_{2.5}$ concentrations measured with the DustTrak were lower than the corresponding values measured with the SidePak (Figure 3). This trend was consistent across the measured concentration range from approximately 10 to >1000 µg/m^3. The mean SidePak/DustTrak $PM_{2.5}$ concentration ratio was 2.15 ± 0.48. These differences can be attributed to technical matters related to the internal setup of the instruments and their factory calibrations. For example, the SidePak inlet has an impactor plate with a specific aerodynamic diameter cut point (here chosen as $PM_{2.5}$), whereas the DustTrak differentiates the particle size based solely on the optical properties of particles.

Following the methodology outlined in Section 2.3, we converted the measured particle number size distributions (via CPC 3007, P-Trak, and AeroTrak) to particle mass size distributions assuming spherical particles of unit density. From integration of the latter, we calculated the $PM_{2.5}$ and PM_{10} concentrations. The calculated $PM_{2.5}$ and PM_{10} concentrations can be compared with those reported by the DustTrak. The calculated $PM_{2.5}$ concentrations were found to be less than those reported by the DustTrak (Figure 4). More variability was observed for PM_{10}, with the calculated PM_{10} both under- and overestimating the DustTrak-derived values across the measured concentration range. The mean calculated-to-DustTrak $PM_{2.5}$ ratio was 0.63 ± 0.58 and that for PM_{10} was 1.46 ± 1.27.

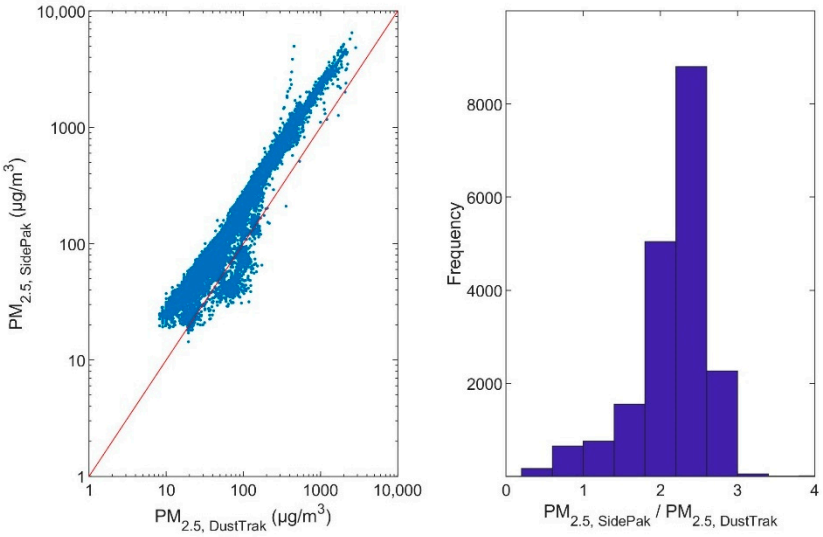

Figure 3. Comparison between the $PM_{2.5}$ concentrations measured with the DustTrak and SidePak.

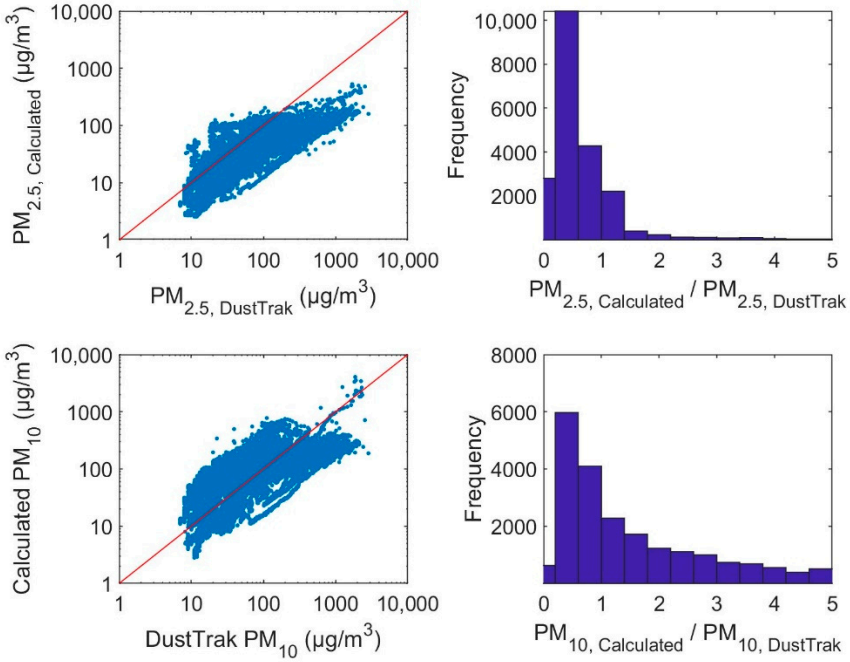

Figure 4. Comparison between the $PM_{2.5}$ and PM_{10} concentrations measured with DustTrak and those calculated using the measured particle number size distributions, assuming spherical particles of unit density.

This brief comparative analysis of the PM concentrations measured by the DustTrak, SidePak, and calculated via measured particle number size distributions illustrates that portable aerosol instruments have limitations and their output is likely to be inconsistent. Relying on a single instrument output may not provide an accurate assessment of PM concentrations. The utilization of an array of portable aerosol instruments can provide lower and upper bounds on PM concentrations in different indoor environments. Calculating PM concentrations from measured particle number size distributions is uncertain in the absence of reliable data on size-resolved particle effective densities for different indoor emission sources.

3.2. Overview of Indoor Particle Concentrations in Jordanian Dwellings

3.2.1. Indoor Particle Concentrations during the Winter Season

An overview of the indoor submicron particle number (PN) concentrations and $PM_{2.5}$ and PM_{10} concentrations is presented Tables 4 and 5 (mean ± SD and 95%) and illustrated in Figure 5 for each of the eight Jordanian dwellings investigated in this study. Particle concentration time series are presented in the supplementary material (Figures S1–S8). Indoor particle concentrations (mean ± SD) were also evaluated during the nighttime, when there were no indoor activities reported in the dwellings and the concentrations were observed to be at their lowest levels (Table 6).

Table 4. Indoor particle number and mass concentrations (mean ± SD and 95%) during the winter campaign.

Site ID	CPC 3007		DustTrak				SidePak	
	PN ($\times 10^4$/cm^3)		$PM_{2.5}$ (μg/m^3)		PM_{10} (μg/m^3)		$PM_{2.5}$ (μg/m^3)	
	Mean ± SD	95%	Mean ± SD	95%	Mean ± SD	95%	Mean ± SD	95%
A1	4.3 ± 6.0	22.6	91 ± 218	612	93 ± 228	628	188 ± 403	1261
A2	1.6 ± 1.7	6.7	44 ± 40	157	47 ± 42	160	–	–
D1	13.3 ± 10.5	30.1	131 ± 202	613	132 ± 202	614	271 ± 448	1446
GFA1	5.4 ± 4.6	22.0	42 ± 26	109	45 ± 30	123	80 ± 38	176
GFA2	3.4 ± 4.0	17.0	29 ± 34	126	29 ± 34	126	–	–
GFA3	6.3 ± 4.8	18.6	433 ± 349	1230	437 ± 350	2140	998 ± 815	2790
H1	11.7 ± 7.4	23.6	138 ± 116	451	141 ± 117	453	325 ± 310	1190
H2	9.7 ± 6.1	25.0	156 ± 190	694	160 ± 190	697	342 ± 477	1690

Table 5. Indoor particle number and mass concentrations (mean ± SD and 95%) during the summer campaign.

Site ID	CPC 3007		DustTrak				SidePak	
	PN ($\times 10^4$/cm^3)		$PM_{2.5}$ (μg/m^3)		PM_{10} (μg/m^3)		$PM_{2.5}$ (μg/m^3)	
	Mean ± SD	95%	Mean ± SD	95%	Mean ± SD	95%	Mean ± SD	95%
GFA2	1.5 ± 1.4	5.5	30 ± 20	62	31 ± 20	64	58 ± 34	104
GFA3	1.9 ± 1.6	6.3	31 ± 46	179	31 ± 46	180	158 ± 216	819
H2	1.6 ± 0.9	3.8	46 ± 24	101	50 ± 26	107	89 ± 64	305

Table 6. Indoor particle number and mass concentrations (mean ± SD) during the nighttime, when there were no reported indoor activities. The concentrations were calculated for the winter campaign only.

Site ID	CPC 3007	DustTrak		SidePak
	PN ($\times 10^3$/cm^3)	$PM_{2.5}$ (μg/m^3)	PM_{10} (μg/m^3)	$PM_{2.5}$ (μg/m^3)
	Mean ± SD	Mean ± SD	Mean ± SD	Mean ± SD
A1	6 ± 3	18 ± 8	18 ± 8	45 ± 19
A2	6 ± 1	10 ± 0	11 ± 1	–
D1	13 ± 2	26 ± 0	26 ± 0	52 ± 3
GFA1	9 ± 1	25 ± 7	26 ± 7	62 ± 15
GFA2	9 ± 3	10 ± 3	10 ± 3	–
GFA3	15 ± 5	67 ± 18	67 ± 18	154 ± 45
H1	10 ± 2	28 ± 6	29 ± 6	59 ± 14
H2	9 ± 2	28 ± 23	29 ± 24	47 ± 28

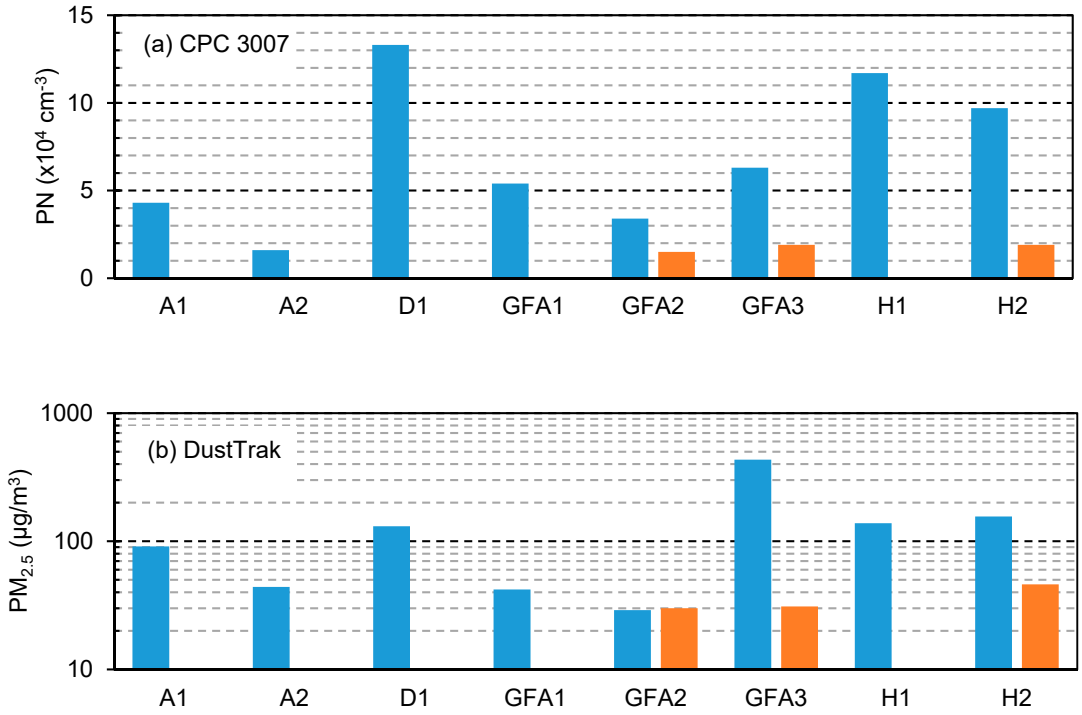

Figure 5. Overall mean indoor particle concentrations during the measurement period in each dwelling: (**a**) submicron particle number (PN) concentrations measured with the condensation particle counter (CPC 3007) and (**b**) $PM_{2.5}$ concentrations measured with the DustTrak. The blue bars represent the winter campaign and the orange bars represent the summer campaign.

Submicron PN concentrations were the lowest in apartment A2, which was equipped with an air conditioning (AC) heating/cooling setting and nonsmoking occupants. For example, the overall mean submicron PN concentrations in A2 was approximately 1.6×10^4 cm^{-3}. The second lowest PN concentrations were observed in the ground floor apartment GFA2, which was equipped with a central heating system (water radiators) and, periodically, electric heaters. Occupants in GFA2 were nonsmokers. The overall mean submicron PN concentration in GFA2 was approximately double that of A2 at 3.2×10^4 cm^{-3}.

The highest submicron PN concentrations were measured in duplex apartment D1, with a mean of 1.3×10^5 cm^{-3}. This apartment had a kerosene heater and one of the occupants smoked shisha (waterpipe or hookah) on a daily basis. The second highest submicron PN concentrations were observed in houses H1 and H2, with overall mean values of 1.2×10^5 cm^{-3} and 9.7×10^4 cm^{-3}, respectively. House H1 was heated by using a natural gas heater and smoking shisha was often conducted by more than one occupant. House H2 was heated with a kerosene heater and cooking activities occurred frequently.

The ground floor apartments, GFA3 and GFA1, showed intermediate submicron PN concentrations among the study sites, with mean concentrations of 6.3×10^4 cm^{-3} and 5.4×10^4 cm^{-3}, respectively. Although occupants in GFA3 heavily smoked tobacco and shisha, the concentrations were lower than those observed in D1 and H1, where shisha was also smoked. The building envelopes of D1 and H1 may be more tightly sealed, with lower infiltration rates compared to GFA3. Furthermore, GFA3 used a natural gas heater and cooking activities were not as frequent. As for GFA1, the heating was a combination of a kerosene heater and a natural gas heater. The cooking activities in GFA1 were minimal and not frequent. Occupants in apartment A1 were nonsmokers. Indoor emission source manipulations were conducted in A1, including various cooking activities and the use of three different types of heating (kerosene heater, natural gas heater, and AC). The overall mean submicron PN concentration in A1 was approximately 4.3×10^4 cm^{-3}.

For $PM_{2.5}$ concentrations, the lowest levels were observed not in A2 (highest submicron PN concentrations), but rather in GFA2, with a mean of approximately 29 $\mu g/m^3$. GFA2 was heated by means of a central heating system and, periodically, with electric heaters. Ground floor apartment GFA1 and apartment A2 exhibited intermediate overall mean $PM_{2.5}$ concentrations among the study sites, with mean values of 42 $\mu g/m^3$ and 44 $\mu g/m^3$, respectively. As previously discussed, the occupants in GFA1 did not conduct frequent cooking activities and heated their dwelling by means of kerosene and natural gas heaters, whereas A2 was heated via an AC. GFA1 was built in the 1970s, whereas A2 was relatively new (less than 10 years old); therefore, A2 is expected to be a more tightly sealed indoor environment compared to GFA1. However, infiltration rate and air leakage (i.e., blower door) measurements were not conducted for the dwellings in this study.

Apartment A1, in which manipulations of various cooking activities and heating methods were conducted, showed an overall mean $PM_{2.5}$ concentration of 91 $\mu g/m^3$. The impact of shisha smoking on $PM_{2.5}$ concentrations in D1 and H1 was clearly evident, with overall mean $PM_{2.5}$ concentrations of 131 $\mu g/m^3$ and 138 $\mu g/m^3$, respectively. The influence of a kerosene heater and intense cooking activities in H2 was also evident, with an overall mean $PM_{2.5}$ concentration of 156 $\mu g/m^3$. The highest $PM_{2.5}$ concentrations were recorded in GFA3 (approximately 433 $\mu g/m^3$), which reflects the frequent shisha and tobacco smoking in this dwelling.

In the absence of indoor activities (Table 6), the submicron PN concentrations were the lowest (approximately 6×10^3 cm^{-3}) in A1 and A2 and the highest in D1 (approximately 1.3×10^4 cm^{-3}) and GFA3 (approximately 1.5×10^4 cm^{-3}). As for the $PM_{2.5}$ concentrations measured with the DustTrak, the lowest concentrations (approximately 10 $\mu g/m^3$) were observed in A2 and GFA2 and the highest concentrations were observed in GFA3 (approximately 67 $\mu g/m^3$). It is important to note that the measured indoor particle concentrations were primarily the result of the transport of outdoor particles indoors via ventilation and infiltration. However, indoor-generated aerosols during the day may still have traces overnight. For example, the dwellings with combustion and smoking activities also had background concentrations higher than other dwellings. Furthermore, differences in background concentrations among dwellings can be due to the geographical location of the dwelling within the city; this might reflect the outdoor aerosol concentrations at a given location [16,48].

3.2.2. Indoor Particle Concentrations: Summer Versus Winter

Indoor aerosol measurements were repeated for three apartments in the summer campaign. We selected a dwelling (H2) that was heated with a kerosene heater and had nonsmoking occupants, a dwelling (GFA2) that was not heated with combustion processes and had nonsmoking occupants, and a dwelling (GFA3) that was heated with a natural gas heater and the occupants were smokers. Although the number of selected indoor environments was fewer in the summer campaign, the measurement period in each dwelling was longer and more extensive than what was measured during the winter campaign.

In general, the observed concentrations during the summer campaign were lower than those observed during the winter campaign (Tables 4 and 5, Figure 5). The overall mean submicron PN concentration during the summer campaign in GFA2 was approximately 1.5×10^4 cm^{-3}, which was about 40% of that during the winter campaign. As for the $PM_{2.5}$ concentrations, the overall mean during the summer campaign was approximately 30 $\mu g/m^3$, which was almost the same as that observed during the winter campaign.

The overall mean submicron PN concentrations in GFA3 and H2 were similar (approximately 1.6–1.9 $\times$ 10^4 cm^{-3}), whereas the corresponding mean $PM_{2.5}$ concentrations were higher in H2 (approximately 46 $\mu g/m^3$) compared to GFA3 (approximately 31 $\mu g/m^3$). The summer/winter ratio for submicron PN concentrations for GFA3 and H2 were 0.3 and 0.2, respectively. The corresponding $PM_{2.5}$ ratios were approximately 0.1 and 0.3. The primary reason for higher particle concentrations during the winter was the use of fossil fuel combustion for heating (i.e., kerosene and natural gas

heaters). Furthermore, the dwellings during the summer were more likely to be better ventilated than during the winter, when the dwellings had to conserve energy during heating periods.

3.3. Indoor Particle Number and Mass Size Distributions in Jordanian Dwellings

3.3.1. Indoor Particle Size Distributions in the Absence of Indoor Activities

The mean particle number and mass size distributions for each dwelling in the absence of indoor activities during the winter campaign are presented in Figure S9. Significant differences in the mean particle number and mass size distributions were observed among the eight dwellings. Based on the number size distributions, the submicron PN concentration was the lowest (approximately 6×10^3 cm^{-3}, with a corresponding $PM_{2.5}$ of 5 $\mu g/m^3$) in dwellings A1 and A2 and the highest in GFA3 (approximately 1.5×10^4 cm^{-3}, with a corresponding $PM_{2.5}$ of 12 $\mu g/m^3$) and D1 (approximately 1.3×10^4 cm^{-3}, with a corresponding $PM_{2.5}$ of 8 $\mu g/m^3$). The mean submicron PN concentration was between 9×10^3 cm^{-3} and 10^4 cm^{-3} and the mean $PM_{2.5}$ was 7–9 $\mu g/m^3$ in the remainder of the dwellings. It should be noted that GFA3 had the highest submicron PN concentration, whereas H2 had the highest $PM_{2.5}$ concentration (approximately 13 $\mu g/m^3$). Differences between the PN and PM concentrations among the eight dwellings is an indicator of variability in the shape and magnitude of the aerosol size distributions, as illustrated in Figure S9.

The coarse PN concentrations were the lowest in A1 (approximately 0.4 cm^{-3}, with a corresponding PM_{coarse} of 0.9 $\mu g/m^3$) and D1 (approximately 0.4 cm^{-3}, with a corresponding PM_{coarse} of 1.3 $\mu g/m^3$) and the highest was in H2 (approximately 5.2 cm^{-3}, with a corresponding PM_{coarse} of 39.9 $\mu g/m^3$) and the second highest was in H1 (approximately 2.5 cm^{-3}, with a corresponding PM_{coarse} of 17.3 $\mu g/m^3$). As for A2, GFA1, and GFA3, the coarse PN concentrations were approximately 0.9 cm^{-3} for each of the dwellings, but the corresponding PM_{coarse} was about 6.3, 3.5, and 5.6 $\mu g/m^3$, respectively. The similarity in the coarse PN concentrations, compared to the differences observed for the PM_{coarse} concentrations, in these dwellings is an indication of differences in the coarse size fraction of the indoor particle size distributions. This likely reflects differences in indoor emission sources of coarse particles among the dwellings. For example, H2 had the highest coarse PN and PM concentrations which could be explained by the existence of pets (more than two cats), in addition to the geographical location of this dwelling, which was close to an arid area in southeast Amman, where dust events and coarse particle resuspension are common.

3.3.2. Overall Mean Indoor Particle Number and Mass Size Distributions

The overall mean particle number and mass size distributions were calculated for each dwelling for the entire winter measurement campaign (Figures 6 and 7). This includes periods with and without indoor activities. In the following section, we will present and discuss the characteristics of the indoor particle number and mass size distributions during different indoor activities. Each dwelling had a unique set of particle number and mass size distributions that reflected the indoor aerosol emission sources associated with the inhabitants' activities, heating processes, and dwelling conditions. For example, among all dwellings, the lowest UFP concentrations were observed in apartment A2 because combustion processes (i.e., cooking using a natural gas stove) were minimal and the indoor space was heated via AC units. GFA2 had the second lowest UFP concentrations because the heating was via water-based central heating and, occasionally, electric heaters. Furthermore, both A2 and GFA2 were nonsmoking dwellings.

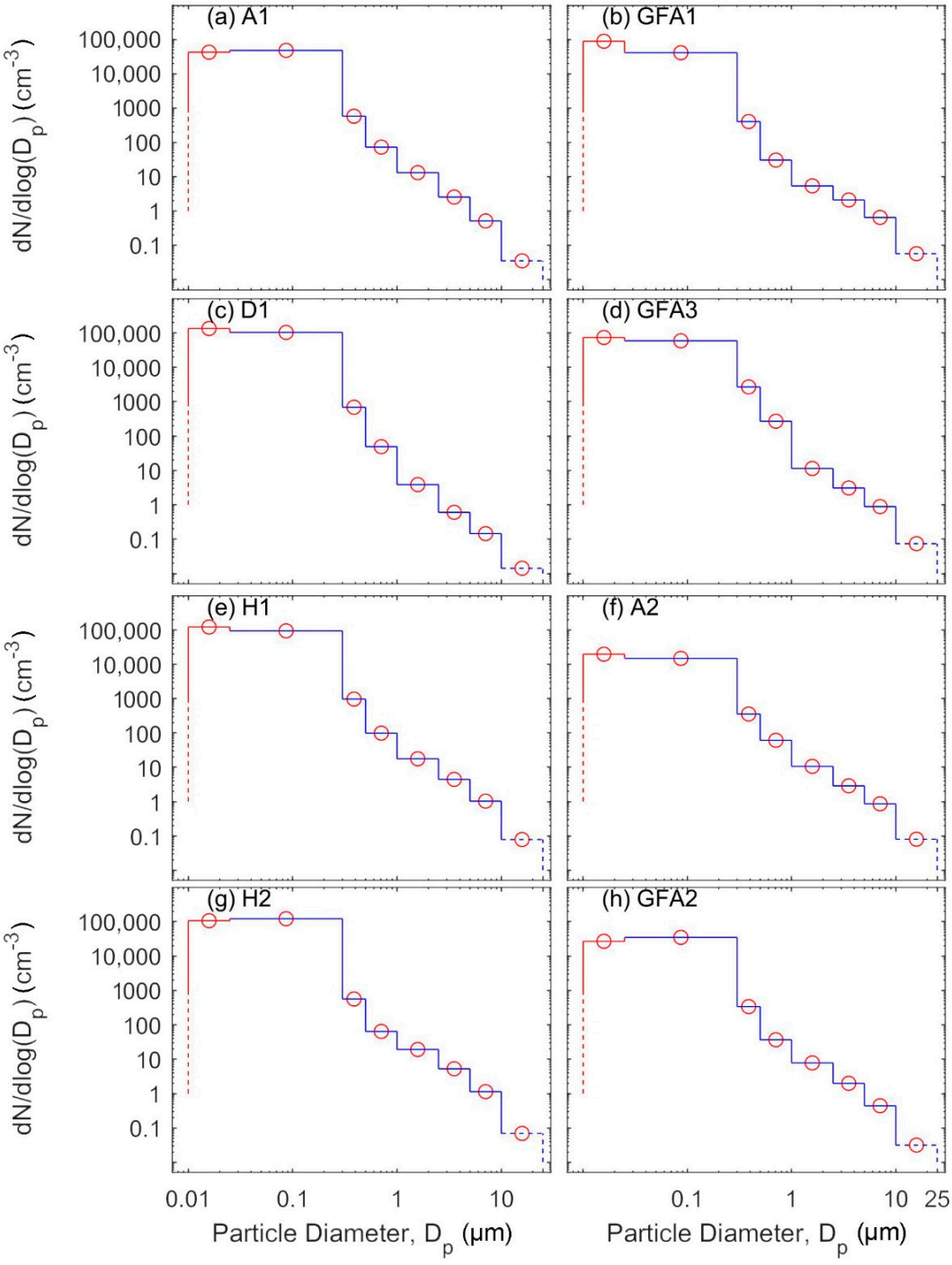

Figure 6. Mean particle number size distributions calculated for the entirety of the winter measurement campaign at each dwelling: (**a**) apartment A1, (**b**) ground floor apartment GFA1, (**c**) duplex D1, (**d**) ground floor apartment GFA3, (**e**) house H1, (**f**) apartment A2, (**g**) house H2, and (**h**) ground floor apartment GFA2.

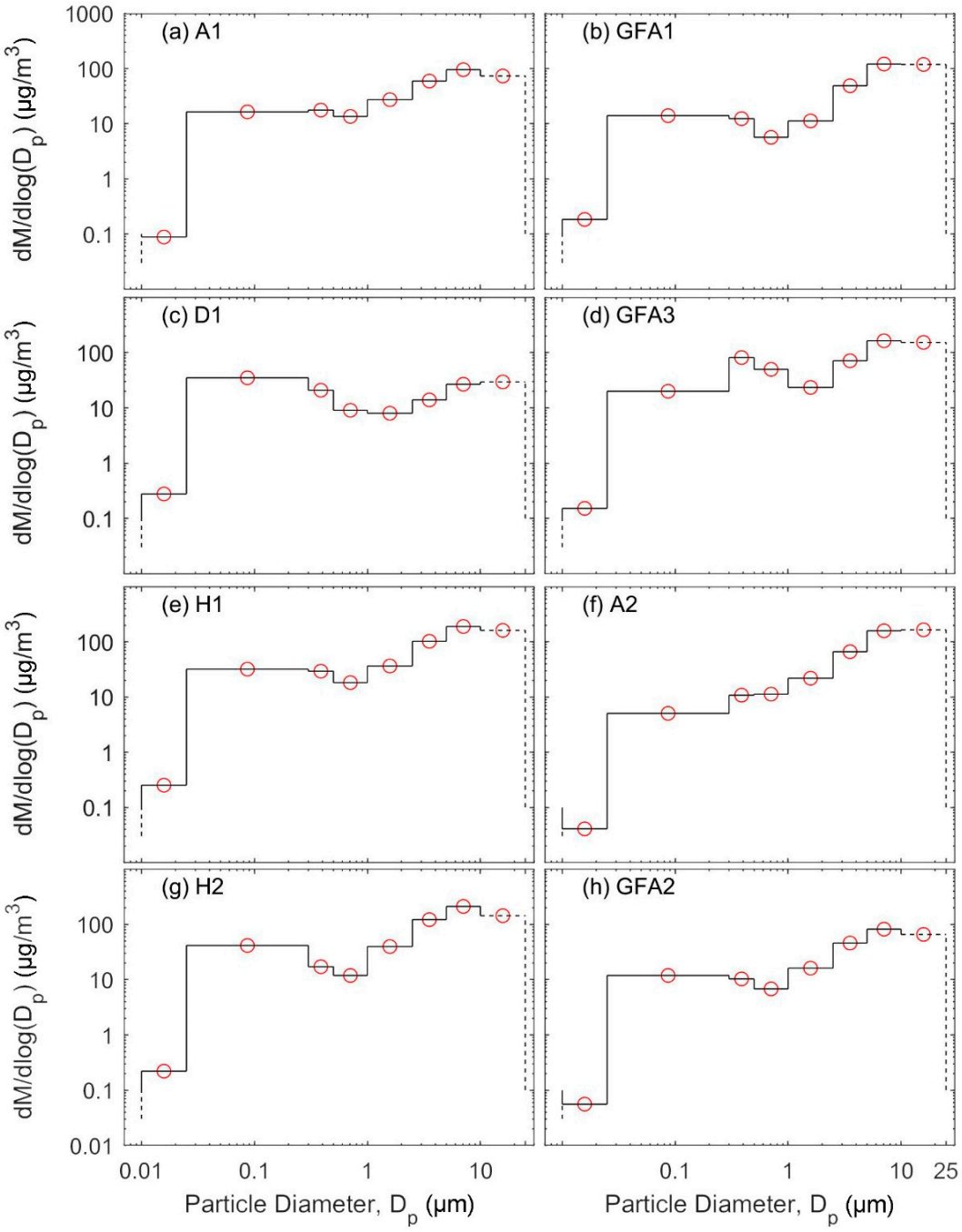

Figure 7. Mean particle mass size distributions calculated for the entirety of the winter measurement campaign at each dwelling: (**a**) apartment A1, (**b**) ground floor apartment GFA1, (**c**) duplex D1, (**d**) ground floor apartment GFA3, (**e**) house H1, (**f**) apartment A2, (**g**) house H2, and (**h**) ground floor apartment GFA2.

Indoor combustion processes had a pronounced impact on submicron particle concentrations, especially UFPs. For example, the impact of using kerosene heaters was evident in A1, D1, GFA1, and H2. Similarly, the impact of using natural gas heaters was evident in A1, GFA1, GFA3, and H1. Shisha smoking was reported in D1, GFA3, and H1, and the impact can be seen in the high concentrations of UFPs that were measured. D1 never obtained a stable background aerosol concentration during the nighttime likely due to traces of the kerosene heater and shisha smoking.

3.3.3. The Impact of Indoor Activities on Indoor Particle Size Distributions and Concentrations

As listed in Table 1, the heating processes reported in this study included both combustion (natural gas heater and/or kerosene heater) and non-combustion (central heating, electric, and air conditioning). The cooking activities were reported on stoves using natural gas. The use of microwaves, coffee machines, and toasters were very rare. Table 7 presents a classification of selected activities and the mean PN and PM concentrations during these activities. The location (i.e., dwelling) and duration of the activities are listed in Table S1. Figures S9–S17 in the supplementary material present the mean particle number and mass size distributions during these activities. In this section, the reported PM concentrations were calculated from the particle mass size distributions by assuming spherical particles of unit density, as previously discussed.

Table 7. Classification of indoor activities and corresponding particle number and mass concentrations. Combustion heating is denoted as (Heat.) and the types are natural gas heater (NG) and kerosene heater (K). Cooking on a natural gas stove is denoted as (Stov.) and smoking cigarettes is denoted by (Cig.).

Combustion		Smoking		Non-Combustion		Additional Activity	$PM_{2.5}$ ($\mu g/m^3$)	PM_{10} ($\mu g/m^3$)	PN_1 ($\times 10^3$ cm^{-3})	PN_{10-1} (cm^{-3})
Heat.	Stov.	Shisha	Cig.	Heat.	Other					
√ (NG)							54 ± 26	64 ± 27	214 ± 71	1 ± 0
√ (NG)	√						70 ± 15	81 ± 17	274 ± 38	4 ± 1
√ (NG)	√					Grill burger/sausage	378 ± 101	2094 ± 882	383 ± 82	131 ± 47
√ (NG)	√						9 ± 2	19 ± 3	85 ± 13	1 ± 0
√ (NG)	√						13 ± 7	16 ± 7	68 ± 11	*null*
√ (NG)	√		√				40 ± 8	189 ± 57	91 ± 18	8 ± 2
√ (NG)	√		√				98 ± 26	158 ± 51	151 ± 37	6 ± 3
√ (NG)	√	√					173 ± 41	424 ± 152	245 ± 53	36 ± 12
√ (NG)	√				√	15 people	65 ± 17	374 ± 91	169 ± 52	13 ± 3
√ (K)	√						130 ± 15	458 ± 110	318 ± 53	27 ± 9
√ (K)	√						82 ± 24	154 ± 60	220 ± 78	7 ± 5
√ (K)	√						78 ± 17	141 ± 36	236 ± 52	5 ± 3
√ (K)	√						43 ± 17	91 ± 60	174 ± 62	5 ± 5
√ (K)	√						99 ± 13	119 ± 14	320 ± 45	1 ± 0
√ (K)	√	√					118 ± 33	139 ± 42	397 ± 60	4 ± 8
√ (K)	√	√					72 ± 24	92 ± 30	330 ± 46	2 ± 1
√ (NG)	√	√×2					139 ± 27	288 ± 114	343 ± 72	15 ± 10
√ (NG)	√	√					75 ± 18	226 ± 76	198 ± 47	14 ± 5
√ (NG)	√	√					61 ± 26	168 ± 60	154 ± 39	8 ± 3
√ (NG)	√	√	√				92 ± 33	189 ± 46	123 ± 34	9 ± 6
√ (NG)	√	√×2	√				132 ± 31	291 ± 61	242 ± 77	13 ± 5
	√					Cooking soup	40 ± 11	76 ± 17	144 ± 40	3 ± 1
	√					Making chai latte	41 ± 13	49 ± 13	160 ± 44	1 ± 0
	√			√ (C)		Intensive cooking	76 ± 41	191 ± 75	116 ± 29	14 ± 10
	√			√ (C)		Intensive cooking	85 ± 32	181 ± 56	207 ± 78	11 ± 3
	√			√ (C)		Intensive cooking	88 ± 31	201 ± 32	183 ± 91	12 ± 2
	√			√ (C)		Making tea	31 ± 10	52 ± 11	117 ± 43	1 ± 0
	√			√ (C)		Making tea + coffee	16 ± 4	42 ± 10	46 ± 13	1 ± 0
	√			√ (AC)		Intensive cooking	62 ± 19	112 ± 40	74 ± 28	11 ± 5
				√ (AC)		AC operation	10 ± 3	61 ± 28	12 ± 4	3 ± 1
				√ (C)	√	Microwave	17 ± 5	44 ± 11	47 ± 17	1 ± 0
					√	Vacuuming	25 ± 7	181 ± 64	47 ± 15	9 ± 3
					√	Brew coffee	7 ± 2	31 ± 21	11 ± 5	1 ± 1
					√	Brew coffee + toast	14 ± 10	18 ± 11	42 ± 29	*null*
					√	Toaster	15 ± 6	23 ± 7	44 ± 21	8 ± 2

Cooking Activities without Combustion Processes

Cooking activities were the most commonly reported indoor emission source in all eight dwellings. Periodically, they were reported in the absence of combustion processes (such as a natural gas stove or heating). The non-combustion cooking activities included: microwave (GFA2, Figure S17), brewing coffee (A1, Figure S10), and toasting bread (A1, Figure S10). When compared to the background concentrations (i.e., in the absence of indoor activities), the concentrations during these activities had a minor impact on the indoor air quality in each dwelling.

Brewing coffee had the smallest impact on indoor aerosol concentrations, with a mean calculated $PM_{2.5}$ concentration of approximately 7 $\mu g/m^3$ (submicron PN concentration of 1.1×10^4 cm^{-3}) and

mean calculated PM_{10} concentration of approximately 31 μg/m^3 (coarse PN concentration of 1 cm^{-3}). Using the toaster doubled the $PM_{2.5}$ concentration and increased the submicron PN concentration four-fold. However, it had a negligible impact on the coarse PN and PM concentrations. Using the microwave had a similar impact on concentrations of fine particles as that observed when using a toaster.

Cooking Activities in the Absence of Combustion Heating Processes

Cooking on a stove (natural gas) can be classified as light or intensive. Light cooking activities were reported in dwelling A1 as cooking soup and making chai latte (Figure S10). During these two activities, the mean calculated $PM_{2.5}$ concentration was approximately 40 μg/m^3. The mean submicron PN concentration was approximately 1.4×10^5 cm^{-3} and 1.6×10^5 cm^{-3} during cooking soup and making chai latte, respectively. The corresponding calculated PM_{10} concentrations were approximately 144 μg/m^3 and 160 μg/m^3 and the coarse PN concentrations were approximately 3 cm^{-3} and 1 cm^{-3}, respectively. Here, the differences in the PM_{10} and coarse PN concentrations were unlikely due to the cooking processes, but rather driven by occupancy and occupant movement-induced particle resuspension near the instruments, which was more intense during cooking soup.

Light cooking activities (such as making tea and/or coffee) were also reported in GFA2, which had a central heating system. During the making of tea and coffee, the mean calculated $PM_{2.5}$ concentrations were approximately 16 μg/m^3 and 31 μg/m^3, respectively (Figure S17). The mean submicron PN concentrations were approximately 1.2×10^5 cm^{-3} and 4.6×10^4 cm^{-3}, respectively. The corresponding calculated PM_{10} concentrations were approximately 52 μg/m^3 and 42 μg/m^3, respectively, and the coarse PN concentrations were about 1 cm^{-3}. This indicates that similar activities might have different impacts on particle concentrations depending on the indoor conditions and the way in which the activity was conducted. For example, variability in dwelling ventilation may play a role, as well as the burning intensity of the natural gas stove.

Intensive cooking activities were reported in dwelling GFA2 (Figure S17, central heating) and A2 (Figure S15, AC heating). Indoor aerosol concentrations during these intensive cooking activities were higher than those observed during light cooking activities (in the absence of combustion heating processes). For example, the mean calculated $PM_{2.5}$ concentrations were between 62 μg/m^3 and 88 μg/m^3. The mean submicron PN concentrations were between 7.4×10^4 cm^{-3} and 2.1×10^5 cm^{-3}. The corresponding mean calculated PM_{10} concentrations were between 112 μg/m^3 and 201 μg/m^3 and the mean coarse PN concentrations were between 3 cm^{-3} and 14 cm^{-3}.

Concurrent Cooking Activities and Combustion Heating Processes

Periodically, the cooking activities occurred concurrently with a combustion heating process (natural gas or kerosene heaters). All of these cooking activities, aside from two, did not report the type of cooking; therefore, it was not possible to classify them as light or intensive cooking. One of the activities was very intensive cooking (grilling burger and sausages) and the other one was a birthday party (candles burning with more than 15 people in the living room). During cooking activities accompanied by a natural gas heater, the mean calculated $PM_{2.5}$ concentrations were between 9 μg/m^3 and 70 μg/m^3 (submicron PN concentrations between 6.8×10^4 cm^{-3} and 2.7×10^5 cm^{-3}). The corresponding mean calculated PM_{10} concentrations were between 16 μg/m^3 and 81 μg/m^3.

Grilling had a significant impact on indoor aerosol concentrations: the mean calculated $PM_{2.5}$ concentration was approximately 378 μg/m^3 (submicron PN concentration of 3.8×10^5 cm^{-3}) and the mean calculated PM_{10} concentration was approximately 2100 μg/m^3 (mean coarse PN concentration of 130 cm^{-3}). The birthday party event had a clear impact on both submicron and micron aerosol concentrations: the mean calculated $PM_{2.5}$ concentration was approximately 65 μg/m^3 (submicron PN concentration of 1.7×10^5 cm^{-3}) and mean calculated PM_{10} concentration was 374 μg/m^3. Using a kerosene heater instead of a natural gas heater further elevated the concentrations of indoor aerosols. During these activities, the mean calculated $PM_{2.5}$ concentrations were between 43 μg/m^3 and 130 μg/m^3

(submicron PN concentration between 1.7×10^5 cm^{-3} and 3.2×10^5 cm^{-3}). The corresponding mean calculated PM_{10} concentrations were between 90 $\mu g/m^3$ and 460 $\mu g/m^3$.

Indoor Smoking of Shisha and Tobacco

Smoking indoors is prohibited in Jordan. However, this is often violated in many indoor environments in the country. In this study, shisha smoking and/or tobacco smoking was reported in three dwellings (GFA3, H1, and D1). It was not possible to separate the smoking events from the combustion processes used for heating or cooking. Therefore, the concentrations reported here were due to a combination of smoking and heating/cooking activities.

Tobacco smoking increased indoor aerosol concentrations as follows: the mean calculated $PM_{2.5}$ concentrations were between 40 $\mu g/m^3$ and 100 $\mu g/m^3$ (submicron PN concentrations between 9×10^4 cm^{-3} and 1.5×10^5 cm^{-3}). The corresponding mean calculated PM_{10} concentrations were between 160 $\mu g/m^3$ and 190 $\mu g/m^3$ (mean coarse PN concentrations between 6 cm^{-3} and 8 cm^{-3}). Shisha smoking had a more pronounced impact on indoor aerosol concentrations compared to tobacco smoking. The mean calculated $PM_{2.5}$ concentrations were between 60 $\mu g/m^3$ and 140 $\mu g/m^3$ (submicron PN concentrations between 1.2×10^5 cm^{-3} and 4×10^5 cm^{-3}). The corresponding mean calculated PM_{10} concentrations were between 90 $\mu g/m^3$ and 290 $\mu g/m^3$ (mean coarse PN concentrations between 2 cm^{-3} and 15 cm^{-3}).

For shisha smoking, the tobacco is mixed with honey (or sweeteners), oil products (such as glycerin), and flavoring products. Charcoal is used as the source of heat to burn the shisha tobacco mixture. Usually, the charcoal is heated up indoors on the stove prior to the shisha smoking event. Shisha and cigarette smoking produces a vast range of pollutants in the form of primary and secondary particulate and gaseous pollution [49–58]. It was also reported that cigarette and shisha smoke may contain compounds of microbiological origin, in addition to hundreds of compounds of known carcinogenicity and inhalation toxicity [49].

3.4. Concentrations of Selected Gaseous Pollutants in Jordanian Dwellings

The indoor activities documented in the eight dwellings were associated with emissions of gaseous pollutants for which exceptionally high concentrations were observed (Figures S1–S8). For example, the shisha smoking and preceding preparation (i.e., charcoal combustion) were associated with CO concentrations that reached as high as 10 ppm in D1 and GFA3. The CO concentrations were further elevated in H1, with concentrations approaching 100 ppm. Emissions of SO_2 were also recorded in D1 during charcoal combustion that accompanied shisha smoking. During shisha smoking, the CO concentrations exceeded the exposure level of 6 ppm due to smoking a single cigarette, as reported by Breland et al. [56], and 2.7 ppm as reported by Eissenberg and Shihadeh [52]. Previous studies have reported CO concentrations in the range of 24–32 ppm during shisha smoking events [51–53].

The eight dwellings exhibited variable concentrations of TVOCs, NO_2, and HCHO. For instance, TVOC concentrations were in the range of 100–1000 ppm in A2 and H2, whereas they were in the range of 1000–10,000 ppm in all ground floor apartments (GFA1, GFA2, and GFA3). NO_2 concentrations were in the range of 0.01–1 ppm in the duplex apartment (D1), ground floor apartments (GFA1, GFA2, and GFA3), and houses (H1 and H2). HCHO concentrations were in the range of 0.01–1 ppm in A2 and GFA1 and reached as high as 5 ppm in H2. O_3 was not detected in any of the dwellings. It should be noted that the gaseous pollutant concentrations presented here are estimates and are likely uncertain due to technical limitations of the low-cost sensing module employed.

3.5. Indoor Versus Outdoor Particle Concentrations

It is important to note that the indoor aerosol measurement periods at each dwelling were short during the winter campaign. Outdoor aerosol measurements were made on a few occasions at each dwelling; however, they were not of sufficient length to make meaningful conclusions about the aerosol indoor-to-outdoor relationship. However, comprehensive measurements of ambient aerosols have

been made in the urban background in Amman [40,41,59–62], for which comparisons with the indoor measurements presented in this study can be made.

In the urban background atmosphere of Amman [62], outdoor PN concentrations were typically higher during the winter compared to the summer; the ratio can be 2–3 based on the daily means. Based on the hourly mean, the outdoor PN concentration had a clear diurnal and weekly pattern, with high concentrations during the workdays, especially during traffic rush hours. For example, the PN concentration diurnal pattern was characterized by two peaks: morning and afternoon. The afternoon peak (wintertime highest concentration range of 3×10^4–3.5×10^4 cm^{-3}) was rather similar on all weekdays; however, the first peak was higher on workdays compared to weekends (wintertime highest concentration range of 4.5×10^4–6.5×10^4 cm^{-3}). The lowest outdoor concentrations were typically observed between 3:00 to 6:00 in the morning, when they are as low as 1.8×10^4 cm^{-3} during the wintertime.

When compared to the results reported in this study (Tables 4–7), the mean indoor PN concentrations were generally higher than those outdoors during the daytime, when indoor activities were taking place. For example, PN concentrations inside all dwellings were less than 1.5×10^4 cm^{-3} between midnight and early morning; i.e., in the absence of indoor activities. However, the overall mean PN concentrations during the winter campaign inside the studied dwellings were in the range of 1.6×10^4–1.3×10^5 cm^{-3}. Looking at the mean concentrations during the indoor activities, the PN concentrations were as high as 4.7×10^4 cm^{-3} during non-combustion cooking activities. During cooking activities conducted on a natural gas stove, the PN concentrations were in the range of 4.6×10^4–3.8×10^5 cm^{-3}. The combination of cooking activities and combustion processes (as the main source of heating) increased the PN concentrations to be in the range of 6.8×10^4–2.7×10^5 cm^{-3}. Grilling sausages and burger indoors was associated with a substantial increase in mean PN concentrations, with levels reaching as high as 3.8×10^5 cm^{-3} ($PM_{2.5}$ = 378 μg/m^3 and PM_{10} = 2094 μg/m^3). Both tobacco and shisha smoking were also associated with significant increases in PN concentrations, with levels reaching 9.1×10^4–4.0×10^5 cm^{-3}.

It is very well documented in the literature that the temporal variation in indoor aerosol concentrations closely follows those outdoors in the absence of indoor activities [20,30,32,63–74]. As such, the aerosol indoor-to-outdoor relationship depends on the size-resolved particle penetration factor for the building envelope, the ventilation and infiltration rates, and the size-resolved deposition rate onto available indoor surfaces [20,30,64]. As can be seen here, and also reported in previous studies, indoor aerosol emission sources, which are closely connected to human activities indoors, produce aerosol concentrations that are usually several times higher than those found outdoors [17,75–77]. Indoor aerosol sources can thus have a significant adverse impact on human health given that people spend the majority of their time indoors [10,11,32].

4. Conclusions

Indoor air quality has been given very little attention in the Middle East. Residential indoor environments in Jordan have unique characteristics with respect to size, ventilation modes, occupancy, activities, cooking styles, and heating processes. These factors vary between the winter and summer. In this study, we reported the results of one of the first comprehensive indoor aerosol measurement campaigns conducted in Jordanian indoor environments. Our methodology was based on the use of portable aerosol instruments covering different particle diameter ranges, from which we could investigate particle number and mass size distributions during different indoor activities. We focused on standard particle size fractions (submicron versus micron, fine versus coarse). The study provides valuable information regarding exposure levels to a wide range of pollutant sources that are commonly found in Jordanian dwellings.

In the absence of indoor activities, indoor PN concentrations varied among the dwellings and were in the range of 6×10^3–1.5×10^4 cm^{-3} (corresponding $PM_{2.5}$ of 5–12 μg/m^3). The coarse PN concentrations were in the range of 0.4–5.2 cm^{-3} (corresponding PM_{coarse} of 0.9–39.9 μg/m^3). Indoor

activities significantly impacted indoor air quality by increasing exposure to particle concentrations that exceeded what could be observed outdoors. Non-combustion cooking activities (microwave, brewing coffee, and toasting bread) had the smallest impact on indoor aerosol concentrations. During such activities, the PN concentrations were in the range of 1.1×10^4–4.7×10^4 cm^{-3}, $PM_{2.5}$ concentrations were in the range of 7–25 $\mu g/m^3$, micron PN concentrations were in the range of 1–9 cm^{-3}, and PM_{10} concentrations were in the range of 44–181 $\mu g/m^3$. Cooking on a natural gas stove had a more pronounced impact on indoor aerosol concentrations compared to non-combustion cooking, with measured PN concentrations in the range of 4.6×10^4–2.1×10^5 cm^{-3}, $PM_{2.5}$ concentrations in the range of 16–88 $\mu g/m^3$, micron PN concentrations in the range of 1–14 cm^{-3}, and PM_{10} concentrations in the range of 42–201 $\mu g/m^3$.

The combination of cooking activities (varying in type and intensity) with heating via combustion of natural gas or kerosene had a significant impact on indoor air quality. PN concentrations were in the range of 6.8×10^4–2.7×10^5 cm^{-3}, $PM_{2.5}$ concentrations were in the range of 9–130 $\mu g/m^3$, micron PN concentrations were in the range of 1–27 cm^{-3}, and PM_{10} concentrations were in the range of 16–458 $\mu g/m^3$. Grilling sausages and burgers indoors was identified as an extreme event, with mean PN concentration reaching 3.8×10^5 cm^{-3}, $PM_{2.5}$ concentrations reaching 378 $\mu g/m^3$, micron PN concentrations reaching 131 cm^{-3}, and PM_{10} concentrations reaching 2094 $\mu g/m^3$.

Both tobacco and shisha smoking adversely impacted indoor air quality in Jordanian dwellings, with the latter being more severe. During tobacco smoking, the PN concentrations were in the range of 9.1×10^4–1.5×10^5 cm^{-3}, $PM_{2.5}$ concentrations were in the range of 40–98 $\mu g/m^3$, micron PN concentrations were in the range of 6–8 cm^{-3}, and PM_{10} concentrations were in the range of 158–189 $\mu g/m^3$. During shisha smoking, the PN concentrations were in the range of 1.2×10^5–4.0×10^5 cm^{-3}, $PM_{2.5}$ concentrations were in the range of 61–173 $\mu g/m^3$, micron PN concentrations were in the range of 2–36 cm^{-3}, and PM_{10} concentrations were in the range of 92–424 $\mu g/m^3$.

The above-mentioned concentration ranges were reported during the winter campaign, when the houses were tightly closed for heating purposes. Indoor aerosol concentrations during the summer campaign were generally lower. The overall mean PN concentrations during the summer campaign were less than 2×10^4 cm^{-3} and $PM_{2.5}$ concentrations were less than 50 $\mu g/m^3$. Some of the reported indoor activities were accompanied with high concentrations of gaseous pollutants. TVOC concentrations exceeded 100 ppm. NO_2 concentrations were in the range of 0.01–1 ppm. HCHO concentrations were in the range of 0.01–5 ppm. During shisha smoking and preceding preparation (e.g., charcoal combustion), the mean CO concentrations reached as high as 100 ppm.

There are a number of limitations of the present study: (1) the measurement periods were short at each dwelling during the winter campaign, (2) the sample population was small (eight dwellings), and (3) outdoor measurements were only conducted on a few occasions for short periods. These limitations can be addressed in future indoor–outdoor measurement campaigns in Jordan. However, indoor aerosol concentrations were compared to long-term outdoor PN measurements conducted in past studies in Jordan.

The results of this study can offer several practical recommendations for improving indoor air quality in Jordanian indoor environments: source control by prohibiting the smoking of tobacco and shisha indoors, improved ventilation during the use of fossil fuel combustion for heating, and cooking with a natural gas stove under a kitchen hood.

Supplementary Materials: The following are available online at http://www.mdpi.com/2073-4433/11/1/41/s1. Table S1: Average particle mass and number concentrations (mean ± stdev) during selected indoor activities. Figure S1: Aerosol concentrations inside apartment A1 during the winter campaign (23–25 December 2018). Figure S2: Aerosol concentrations inside ground floor apartment GFA1 during the winter campaign (25–27 December 2018). Figure S3: Aerosol concentrations inside duplex apartment D1 during the winter campaign (28–30 December 2018). Figure S4: Aerosol concentrations inside ground floor apartment GFA3 during the winter campaign (31 December 2018–2 January 2019). Figure S5: Aerosol concentrations inside house H1 during the winter campaign (2–4 January 2019). Figure S6: Aerosol concentrations inside apartment A2 during the winter campaign (4–5 January 2019). Figure S7: Aerosol concentrations inside house H2 during the winter campaign (6–9 January 2019). Figure S8: Aerosol concentrations inside ground floor apartment GFA2 during the winter campaign (9–12 January

2019). Figure S9: Mean particle number size distributions and corresponding particle mass size distributions in the absence of indoor activities during the winter campaign at each study site. Figure S10: Mean particle number size distributions and particle mass size distributions during selected activities reported inside Apartment A1 during the winter campaign (23–25 December2018). Figure S11: Mean particle number size distributions and particle mass size distributions during selected activities reported inside ground floor apartment GFA1 during the winter campaign (25–27 December 2018). Figure S12: Mean particle number size distributions and particle mass size distributions during selected activities reported inside duplex D1 during the winter campaign (28–30 December 2018). Figure S13: Mean particle number size distributions and particle mass size distributions during selected activities reported inside ground floor apartment GFA3 during the winter campaign (31 December 2018–2 January 2019). Figure S14: Mean particle number size distributions and particle mass size distributions during selected activities reported inside house H1 during the winter campaign (2–4 January 2019). Figure S15: Mean particle number size distributions and particle mass size distributions during selected activities reported inside apartment A2 during the winter campaign (4–5 January 2019). Figure S16: Mean particle number size distributions and particle mass size distributions during selected activities reported inside house H2 during the winter campaign (6–9 January 2019). Figure S17: Mean particle number size distributions and particle mass size distributions during selected activities reported inside ground floor apartment GFA2 during the winter campaign (9–12 January 2019).

Author Contributions: Conceptualization, T.H., M.M., A.A.-H., and O.A.; methodology, T.H., O.J., K.A., A.A., and O.A.; validation, T.H.; formal analysis, T.H., O.J., and A.A.; investigation, T.H.; resources, T.H. and M.M.; data curation, T.H., O.J., K.A., and A.A.; writing—original draft preparation, T.H. and A.A.-H.; writing—review and editing, T.H., B.E.B., A.J.K., J.L., M.M., and A.A.-H.; visualization, T.H.; supervision, T.H. and A.A.-H.; project administration, T.H. and A.A.-H.; funding acquisition, T.H. and M.M. All authors have read and agreed to the published version of the manuscript.

Funding: This research was funded by the World Health Organization regional office in Amman. The research infrastructure utilized in this project was partly funded by the Deanship of Academic Research (DAR, project number 1516) at the University of Jordan and the Scientific Research Support Fund (SRF, project number BAS-1-2-2015) at the Jordanian Ministry of Higher Education. This research was part of a close collaboration between the University of Jordan and the Institute for Atmospheric and Earth System Research (INAR/Physics, University of Helsinki) via the Academy of Finland Center of Excellence (project No. 272041 and 1307537).

Acknowledgments: The first author would like to thank the occupants for allowing the indoor measurement campaigns to be conducted in their dwellings. Some of them also helped in follow-up aerosol measurements and reporting of indoor activities. This manuscript was written and completed during the sabbatical leave of the first author (T.H.) that was spent at the University of Helsinki and supported by the University of Helsinki during 2019. Open access funding was provided by the University of Helsinki.

Conflicts of Interest: The authors declare no conflict of interest.

References

1. World Health Organization (WHO). Ambient Air Pollution: A Global Assessment of Exposure and Burden of Disease. 2016. Available online: http://apps.who.int/iris/bitstream/10665/250141/1/9789241511353-eng.pdf?ua=1 (accessed on 3 December 2019).
2. World Health Organization (WHO). Household Air Pollution and Health. 2018. Available online: https://www.who.int/news-room/fact-sheets/detail/household-air-pollution-and-health (accessed on 3 December 2019).
3. Health Effects Institute (HEI). State of Global Air. In *Special Report*; Health Effects Institute: Boston, MA, USA, 2017.
4. World Health Organization (WHO). The Right to Healthy Indoor Air. 2000. Available online: http://www.euro.who.int/en/health-topics/environment-and-health/air-quality/publications/pre2009/the-right-to-healthy-indoor-air (accessed on 3 December 2019).
5. Odeh, I.; Hussein, T. Activity pattern of urban adult students in an Eastern Mediterranean Society. *Int. J. Environ. Res. Public Health* **2016**, *13*, 960. [CrossRef] [PubMed]
6. Hussein, T.; Paasonen, P.; Kulmala, M. Activity pattern of a selected group of school occupants and their family members in Helsinki-Finland. *Sci. Total Environ.* **2012**, *425*, 289–292. [CrossRef] [PubMed]
7. Schwerizer, C.; Edwards, R.; Bayer-Oglesby, L.; Gauderman, W.; Ilacqua, V.; Jantunen, M.; Lai, H.K.; Nieuwenhuijsen, M.; Künzli, N. Indoor time-microenvironment-activity patterns in seven regions of Europe. *J. Expo. Sci. Environ. Epidemiol.* **2007**, *17*, 170–181. [CrossRef]
8. Klepeis, N.E.; Nelson, W.C.; Ott, W.R.; Robinson, J.P.; Tsang, A.M.; Switzer, P.; Behar, J.V.; Hem, S.C.; Engelmann, W.H. The national human activity pattern survey NHAPS: A resource for assessing exposure to environmental pollutants. *J. Expo. Anal. Environ. Epidemiol.* **2001**, *11*, 231–252. [CrossRef] [PubMed]

9. McCurdy, T.; Glen, G.; Smith, L.; Lakkadi, Y. The National Exposure Research Laboratory's Consolidated Human Activity Database. *J. Expo. Anal. Environ. Epidemiol.* **2000**, *10*, 566–578. [CrossRef] [PubMed]
10. Koivisto, A.J.; Kling, K.I.; Hänninen, O.; Jayjock, M.; Löndahl, J.; Wierzbicka, A.; Fonseca, A.S.; Uhrbrand, K.; Boor, B.E.; Jiménez, A.S.; et al. Source specific exposure and risk assessment for indoor aerosols. *Sci. Total Environ.* **2019**, *668*, 13–24. [CrossRef] [PubMed]
11. Jones, A.P. Indoor air quality and health. *Atmos. Environ.* **1999**, *33*, 4535–4564. [CrossRef]
12. Streets, D.G.; Yan, F.; Chin, M.; Diehl, T.; Mahowald, N.; Schultz, M.; Wild, M.; Wu, Y.; Yu, C. Anthropogenic and natural contributions to regional trends in aerosol optical depth, 1980–2006. *J. Geophys. Res.* **2009**, *114*, D00D18. [CrossRef]
13. Karagulian, F.; Belis, C.A.; Francisco, C.; Dora, C.; Prüss-Ustün, A.M.; Bonjour, S.; Adair-Rohani, H.; Amann, M. Contributions to cities' ambient particulate matter (PM)—A systematic review of local source contributions at global level. *Atmos. Environ.* **2015**, *120*, 475–483. [CrossRef]
14. Abadie, M.O.; Blondeau, P. PANDORA database: A compilation of indoor air pollutant emissions. *HVAC&R Res.* **2011**, *17*, 602–613.
15. Boor, B.E.; Spilak, M.P.; Laverge, J.; Novoselac, A.; Xu, Y. Human exposure to indoor air pollutants in sleep microenvironments: A literature review. *Build. Environ.* **2017**, *125*, 528–555. [CrossRef]
16. Chen, C.; Zhao, B. Review of relationship between indoor and outdoor particles: I/O ratio, infiltration factor and penetration factor. *Atmos. Environ.* **2011**, *45*, 275–288. [CrossRef]
17. Hussein, T.; Wierzbicka, A.; Löndahl, J.; Lazaridis, M.; Hänninen, O. Indoor aerosol modeling for assessment of exposure and respiratory tract deposited dose. *Atmos. Environ.* **2015**, *106*, 402–411. [CrossRef]
18. Koivisto, J.; Hussein, T.; Niemelä, R.; Tuomi, T.; Hämeri, K. Impact of particle emissions of new laser printers on a modeled office room. *Atmos. Environ.* **2010**, *44*, 2140–2146. [CrossRef]
19. Lin, C.-H.; Lo, P.-Y.; Wu, H.-D.; Chang, C.; Wang, L.-C. Association between indoor air pollution and respiratory disease in companion dogs and cats. *J. Vet. Intern. Med.* **2018**, *32*, 1259–1267. [CrossRef] [PubMed]
20. Morawska, L.; Afshari, A.; Bae, G.N.; Buonanno, G.; Chao, C.Y.H.; Hänninen, O.; Hofmann, W.; Isaxon, C.; Jayaratne, E.R.; Pasanen, P.; et al. Indoor aerosols: From personal exposure to risk assessment. *Indoor Air* **2013**, *23*, 462–487. [CrossRef] [PubMed]
21. Morawska, L.; He, C.; Johnson, G.; Jayaratne, R.; Salthammer, T.; Wang, H.; Uhde, E.; Bostrom, T.; Modini, R.; Ayoko, G.; et al. An Investigation into the characteristics and formation mechanisms of particles originating from the operation of laser printers. *Environ. Sci. Technol.* **2009**, *43*, 1015–1022. [CrossRef]
22. Sangiorgi, G.; Ferrero, L.; Ferrini, B.S.; Lo Porto, C.; Perrone, M.G.; Zangrando, R.; Gambaro, A.; Lazzati, Z.; Bolzacchini, E. Indoor airborne particle sources and semi-volatile partitioning effect of outdoor fine PM in offices. *Atmos. Environ.* **2013**, *65*, 205–214. [CrossRef]
23. Wensing, M.; Schripp, T.; Uhde, E.; Salthammer, T. Ultra-fine particles release from hardcopy devices: Sources, real-room measurements and efficiency of filter accessories. *Sci. Total Environ.* **2008**, *407*, 418–427. [CrossRef]
24. He, C.; Morawska, L.; Hitchins, J.; Gilbert, D. Contribution from indoor sources to particle number and mass concentrations in residential houses. *Atmos. Environ.* **2004**, *38*, 3405–3415. [CrossRef]
25. He, C.; Morawska, L.; Taplin, L. Particle emission characteristics of office printers. *Environ. Sci. Technol.* **2007**, *41*, 6039–6045. [CrossRef] [PubMed]
26. Ren, Y.; Cheng, T.; Chen, J. Polycyclic aromatic hydrocarbons in dust from computers: One possible indoor source of human exposure. *Atmos. Environ.* **2006**, *40*, 6956–6965. [CrossRef]
27. Afshari, A.; Matson, U.; Ekberg, L.E. Characterization of indoor sources of fine and ultrafine particles: A study conducted in a full-scale chamber. *Indoor Air* **2005**, *15*, 141–150. [CrossRef] [PubMed]
28. Weschler, C.J. Changes in indoor pollutants since the 1950s. *Atmos. Environ.* **2009**, *43*, 153–169. [CrossRef]
29. Madanat, H.; Barnes, M.D.; Cole, E.C. Knowledge of the effects of indoor air quality on health among women in Jordan. *Health Educ. Behav.* **2008**, *35*, 105–118. [CrossRef] [PubMed]
30. Hussein, T. Particle size distributions inside a university office in Amman, Jordan. *Jordan J. Phys.* **2014**, *7*, 73–83.
31. Hussein, T.; Dada, L.; Juwhari, H.; Faouri, D. Characterization, fate, and re-suspension of aerosol particles (0.3–10 μm): The effects of occupancy and carpet use. *Aerosol Air Qual. Res.* **2015**, *15*, 2367–2377. [CrossRef]

32. Hussein, T. Indoor-to-Outdoor relationship of aerosol particles inside a naturally ventilated apartment—A comparison between single-parameter analysis and indoor aerosol model simulation. *Sci. Total Environ.* **2017**, *596–597*, 321–330. [CrossRef]
33. Wang, Y.; Xing, Z.; Zhao, S.; Zheng, M.; Mu, C.; Du, K. Are emissions of black carbon from gasoline vehicles overestimated? Real-time, in situ measurement of black carbon emission factors. *Sci. Total Environ.* **2016**, *547*, 422–428. [CrossRef]
34. Jiang, R.T.; Acevedo-Bolton, V.; Cheng, K.C.; Klepeis, N.E.; Ott, W.R.; Hildemann, L.M. Determination of response of real-time SidePak AM510 monitor to secondhand smoke, other common indoor aerosols, and outdoor aerosol. *J. Environ. Monit.* **2011**, *13*, 1695–1702. [CrossRef]
35. Matson, U.; Ekberg, L.E.; Afshari, A. Measurement of ultrafine particles: A comparison of two handheld condensation particle counters. *Aerosol Sci. Technol.* **2004**, *38*, 487–495. [CrossRef]
36. Lin, C.; Gillespie, J.; Schuder, M.D.; Duberstein, W.; Beverland, I.J.; Heal, M.R. Evaluation and calibration of Aeroqual series 500 portable gas sensors for accurate measurement of ambient ozone and nitrogen dioxide. *Atmos. Environ.* **2015**, *100*, 111–116. [CrossRef]
37. Cai, J.; Yan, B.; Ross, J.; Zhang, D.; Kinney, P.L.; Perzanowski, M.S.; Jung, K.; Miller, R.; Chillrud, S.N. Validation of MicroAeth® as a black carbon monitor for fixed-site measurement and optimization for personal exposure characterization. *Aerosol Air Qual. Res.* **2014**, *14*, 1–9. [CrossRef] [PubMed]
38. Cheng, Y.H.; Lin, M.H. Real-time performance of the micro-aeth AE51 and the effects of aerosol loading on its measurement results at a traffic site. *Aerosol Air Qual. Res.* **2013**, *13*, 1853–1863. [CrossRef]
39. Chung, A.; Chang, D.P.Y.; Kleeman, M.J.; Perry, K.; Cahill, T.A.; Dutcher, D.; McDougal, E.M.; Stroud, K. Comparison of real-time instruments used to monitor airborne particulate matter. *J. Air Waste Manag. Assoc.* **2001**, *51*, 109–120. [CrossRef] [PubMed]
40. Hussein, T.; Boor, B.E.; Dos Santos, V.N.; Kangasluoma, J.; Petäjä, T.; Lihavainen, H. Mobile aerosol measurement in the eastern Mediterranean—A utilization of portable instruments. *Aerosol Air Qual. Res.* **2017**, *17*, 1775–1786. [CrossRef]
41. Hussein, T.; Saleh, S.S.A.; dos Santos, V.N.; Abdullah, H.; Boor, B.E. Black carbon and particulate matter concentrations in eastern Mediterranean urban conditions—An assessment based on integrated stationary and mobile observations. *Atmosphere* **2019**, *10*, 323. [CrossRef]
42. Hämeri, K.; Koponen, I.K.; Aalto, P.P.; Kulmala, M. The particle detection efficiency of the TSI3007 condensation particle counter. *Aerosol Sci.* **2002**, *33*, 1463–1469. [CrossRef]
43. Maricq, M.M. Monitoring motor vehicle PM emissions: An evaluation of three portable low-cost aerosol instruments. *Aerosol Sci. Technol.* **2013**, *47*, 564–573. [CrossRef]
44. Nyarku, M.; Mazaheri, M.; Jayaratne, R.; Dunbabin, M.; Rahman, M.M.; Uhde, E.; Morawska, L. Mobile phones as monitors of personal exposure to air pollution: Is this the future? *PLoS ONE* **2018**, *13*, e0193150. [CrossRef]
45. Wang, X.; Chancellor, G.; Evenstad, J.; Farnsworth, J.; Hase, A.; Olson, G.; Sreenath, A.; Agarwal, J. A novel optical instrument for estimating size segregated aerosol mass concentration in real time. *Aerosol Sci. Technol.* **2009**, *43*, 939–950. [CrossRef]
46. Viana, M.; Rivas, I.; Reche, C.; Fonseca, A.S.; Pérez, N.; Querol, X.; Alastuey, A.; Álvarez-Pedrerol, M.; Sunyer, J. Field comparison of portable and stationary instruments for outdoor urban air exposure assessments. *Atmos. Environ.* **2015**, *123*, 220–228. [CrossRef]
47. Hussein, T.; Saleh, S.S.A.; dos Santos, V.N.; Boor, B.E.; Koivisto, A.J.; Löndahl, J. Regional inhaled deposited dose of urban aerosols in an eastern Mediterranean city. *Atmosphere* **2019**, *10*, 530. [CrossRef]
48. Huang, L.; Pui, Z.; Sundell, J. Characterizing the indoor-outdoor relationship of fine particulate matter in non-heating season for urban residences in Beijing. *PLoS ONE* **2015**, *10*, e0138559. [CrossRef]
49. Markowicz, P.; Löndahl, J.; Wierzbicka, A.; Suleiman, R.; Shihadeh, A.; Larsson, L. A study on particles and some microbial markers in waterpipe tobacco smoke. *Sci. Total Environ.* **2014**, *499*, 107–113. [CrossRef]
50. Daher, N.; Saleh, R.; Jaroudi, E.; Sheheitli, H.; Badr, T.; Sepetdjian, E.; Al Rashidi, M.; Saliba, N.; Shihadeh, A. Comparison of carcinogen, carbon monoxide, and ultrafine particle emissions from narghile waterpipe and cigarette smoking: Sidestream smoke measurements and assessment of second-hand smoke emission factors. *Atmos. Environ.* **2010**, *44*, 8–14. [CrossRef]
51. Maziak, W.; Rastam, S.; Ibrahim, I.; Ward, K.D.; Shihadeh, A.; Eissenberg, T. CO exposure, puff topography, and subjective effects in waterpipe tobacco smokers. *Nicotine Tobacco Res.* **2009**, *11*, 806–811. [CrossRef]

52. Eissenberg, T.; Shihadeh, A. Waterpipe tobacco and cigarette smoking direct comparison of toxicant exposure. *Am. J. Prev. Med.* **2009**, *37*, 518–523. [CrossRef]
53. El-Nachef, W.N.; Hammond, S.K. Exhaled carbon monoxide with waterpipe use in US students. *JAMA* **2008**, *299*, 36–38. [CrossRef]
54. Al Rashidi, M.; Shihadeh, A.; Saliba, N.A. Volatile aldehydes in the mainstream smoke of the narghile waterpipe. *Food Chem. Toxicol.* **2008**, *46*, 3546–3549. [CrossRef]
55. Sepetdjian, E.; Alan Shihadeh, A.; Saliba, N.A. Measurement of 16 polycyclic aromatic hydrocarbons in narghile waterpipe tobacco smoke. *Food Chem. Toxicol.* **2008**, *46*, 1582–1590. [CrossRef] [PubMed]
56. Breland, A.B.; Kleykamp, B.A.; Eissenberg, T. Clinical laboratory evaluation of potential reduced exposure products for smokers. *Nicotine Tobacco Res.* **2006**, *8*, 727–738. [CrossRef] [PubMed]
57. Shihadeh, A.; Saleh, R. Polycyclic aromatic hydrocarbons, carbon monoxide, "tar", and nicotine in the mainstream smoke aerosol of the narghile water pipe. *Food Chem. Toxicol.* **2005**, *43*, 655–661. [CrossRef] [PubMed]
58. Shihadeh, A. Investigation of mainstream smoke aerosol of the argileh water pipe. *Food Chem. Toxicol.* **2003**, *41*, 143–152. [CrossRef]
59. Hussein, T.; Halayka, M.; Abu Al-Ruz, R.; Abdullah, H.; Mølgaard, B.; Petäjä, T. Fine particle number concentrations in Amman and Zarqa during spring 2014. *Jordan J. Phys.* **2016**, *9*, 31–46.
60. Hussein, T.; Rasha, A.; Tuukka, P.; Heikki, J.; Arafah, D.; Kaarle, H.; Markku, K. Local air pollution versus short-range transported dust episodes: A comparative study for submicron particle number concentration. *Aerosol Air Qual. Res.* **2011**, *11*, 109–119. [CrossRef]
61. Saleh, S.S.A.; Shilbayeh, Z.; Alkattan, H.; Al-Refie, M.R.; Jaghbeir, O.; Hussein, T. Temporal variations of submicron particle number concentrations at an urban background site in Amman—Jordan. *Jordan J. Earth Environ. Sci.* **2019**, *10*, 37–44.
62. Hussein, T.; Dada, L.; Hakala, S.; Petäjä, T.; Kulmala, M. Urban aerosols particle size characterization in eastern Mediterranean conditions. *Atmosphere* **2019**, *10*, 710. [CrossRef]
63. Hussein, T.; Kulmala, M. Indoor aerosol modeling: Basic principles and practical applications. *Water Air Soil Pollut. Focus* **2008**, *8*, 23–34. [CrossRef]
64. Nazaroff, W.W. Indoor particle dynamics. *Indoor Air* **2004**, *14*, 175–183. [CrossRef]
65. Wierzbicka, A.; Bohgard, M.; Pagels, J.H.; Dahl, A.; Löndahl, J.; Hussein, T.; Swietlicki, E.; Gudmundsson, A. Quantification of differences between occupancy and total monitoring periods for better assessment of exposure to particles in indoor environments. *Atmos. Environ.* **2015**, *106*, 419–428. [CrossRef]
66. Buonanno, G.; Fuoco, F.C.; Marini, S.; Stabile, L. Particle re-suspension in school gyms during physical activities. *Aerosol Air Qual. Res.* **2012**, *12*, 803–813. [CrossRef]
67. Hussein, T.; Hämeri, K.; Kulmala, M. Long-term indoor-outdoor aerosol measurement in Helsinki, Finland. *Boreal Environ. Res.* **2002**, *7*, 141–150.
68. Shaughnessy, R.; Vu, H. Particle loadings and resuspension related to floor coverings in chamber and in occupied school environments. *Atmos. Environ.* **2012**, *55*, 515–524. [CrossRef]
69. Hussein, T.; Hämeri, K.; Aalto, P.; Asmi, A.; Kakko, L.; Kulmala, M. Particle size characterization and the indoor-to-outdoor relationship of atmospheric aerosols in Helsinki. *Scand. J. Work Health Environ.* **2004**, *30* (Suppl. 2), 54–62.
70. Ferro, A.R.; Kopperund, R.J.; Hildemann, L.M. Source strengths for indoor human activities that resuspend particulate matter. *Environ. Sci. Technol.* **2004**, *38*, 1759–1764. [CrossRef]
71. Hussein, T.; Korhonen, H.; Herrmann, E.; Hämeri, K.; Lehtinen, K.; Kulmala, M. Emission rates due to indoor activities: Indoor aerosol model development, evaluation, and applications. *Aerosol Sci. Technol.* **2005**, *39*, 1111–1127. [CrossRef]
72. Kubota, Y.; Higuchi, H. Aerodynamic Particle re-suspension due to human foot and model foot motions. *Aerosol Sci. Technol.* **2013**, *47*, 208–217. [CrossRef]
73. Hirsikko, A.; Kulmala, M.; Yli-Juuti, T.; Nieminen, T.; Hussein, T.; Vartiainen, E.; Laakso, L. Indoor and outdoor air ion and particle number size distributions in the urban background atmosphere of Helsinki, Finland. *Boreal Environ. Res.* **2007**, *12*, 295–310.
74. Lazaridis, M.; Eleftheriadis, K.; Ždímal, V.; Schwarz, J.; Wagner, Z.; Ondráček, J.; Drossinos, Y.; Glytsos, T.; Vratolis, S.; Torseth, K.; et al. Number concentrations and modal structure of indoor/outdoor fine particles in four European Cities. *Aerosol Air Qual. Res.* **2017**, *17*, 131–146. [CrossRef]

75. Hussein, T.; Hämeri, K.; Heikkinen, M.S.A.; Kulmala, M. Indoor and outdoor particle size characterization at a family house in Espoo—Finland. *Atmos. Environ.* **2005**, *39*, 3697–3709. [CrossRef]
76. Hussein, T.; Glytsos, T.; Ondráček, J.; Ždímal, V.; Hämeri, K.; Lazaridis, M.; Smolik, J.; Kulmala, M. Particle size characterization and emission rates during indoor activities in a house. *Atmos. Environ.* **2006**, *40*, 4285–4307. [CrossRef]
77. Maragkidou, A.; Jaghbeir, O.; Hämeri, K.; Hussein, T. Aerosol particles (0.3–10 μm) inside an educational workshop-emission rate and inhaled deposited dose. *Build. Environ.* **2018**, *140*, 80–89. [CrossRef]